

Spin Dependent Transport in Carbon Nanostructures

B. Montanari^b, and N. M. Harrison^{a,b}

^aThomas Young Centre, Department of Chemistry,
Imperial College London, Exhibition Road, London, SW7 2AZ, United Kingdom

^bComputational Science and Engineering Department, STFC Rutherford Appleton Laboratory,
Didcot, Oxon, OX11 0QX, United Kingdom
barbara.montanari@stfc.ac.uk, nicholas.harrison@imperial.ac.uk

ABSTRACT

Keywords: graphene, transport, spintronics, theory, magnetism

1 INTRODUCTION

For the past fifty years progress in the miniaturisation of silicon devices has produced an exponential growth in performance but quantum limits are now being reached as transistor gate lengths approach 5nm. The exploitation of electron spin rather than charge for information storage and manipulation (*spintronics*) has the potential for efficient operation on the sub 1nm length scale and thus to facilitate another generation of devices. In order to achieve this a readily available spin injection material is required; ideally, a material that is a semiconductor, ferromagnetic at room temperature, with a highly tunable band gap and magnetic coupling. The controlled synthesis of such a material has not yet been achieved.

The occurrence of ferromagnetism in purely *sp*-bonded systems provides a challenge to theoretical physics and an opportunity to generate a new class of materials that may be of great value for spintronics.

In the current work hybrid exchange density functional theory is used to demonstrate that local spin moment formation can occur in graphene sheets at both localised and extended defects. In addition, the localised moments are strongly coupled via a spin polarisation of the sheet which, under particular circumstances, is sufficient to produce a ferromagnetic state stable at ambient temperatures. The resultant optical energy gap and magnetic coupling are sensitive to the scale of the nanostructure, the arrangement and concentration of defects; this suggests a mechanism for the tuning of magnetic and electronic properties for specific device applications.

2 METHODOLOGY

Spin localisation at local and extended defects and long range magnetic coupling are studied here using hybrid exchange density functional theory (B3LYP [1]) which significantly extends the reliability of the widely used local and gradient corrected approximations to density functional theory in strongly interacting systems [2].

In particular the energy gap and the tendency to electron localisation in extended systems are well described. All calculations are performed using the CRYSTAL implementation [3] in which the all electron periodic crystalline wavefunctions are expanded as a linear combination of atom centred Gaussian orbitals (LCAO) with *s*, *p*, *d*, or *f* symmetry. This approach is particularly suitable for use with hybrid functionals as the Fock exchange can be computed reliably and efficiently. Basis sets of double valence quality (6-21G* for C and 6-31G* for H) are used. A reciprocal space sampling on a Pack-Monkhorst grid of shrinking factor 6 is adopted which is sufficient to converge the total energy to within 10⁻⁴ eV per unit cell. The energies of various magnetic states have been generated by constraining the initial spin density matrix and then seeking stationary points of the self consistent field procedure.

The graphene sheet is a planar lattice of carbon atoms arranged as edge sharing hexagons which is defined by a unit cell containing two atoms each of which is a member of a distinct sublattice; an arrangement referred to as a bipartite lattice. The bonding of the sheet is *sp*² with each carbon atom σ bonded to three neighbours in the plane and contributing one electron to a delocalised, half filled, π -electron band.

In the present work extended defects are studied by considering ribbons of graphene cut from this sheet and local defects by considering carbon vacancies. In both cases the key issue is the behaviour of the π -electrons and so σ bonds are, where sterically possible, simply saturated by hydrogen atoms. These defects are chosen as representative examples and their behaviour is here taken to be representative of the many different types of defect that can be generated in graphene nanostructures.

The optimised structure of the sheets has a lattice constant of 2.460 Å, 0.04% smaller than the observed lattice constant of natural graphite and corresponding to a C-C bond length of 1.420 Å.

3 GRAPHENE RIBBONS

A graphene ribbon was obtained by cutting a graphene sheet along two parallel zig-zag lines and saturating the σ -bonds of the edges with H atoms, figure 1. The rib-

bon is periodic in the x direction only; the periodic unit cell is delimited by dashed lines in the figure. The width of the ribbon along the non periodic dimension y , is defined here by the number, N , of *trans*-polyacetylene-like rows of carbon atoms that run along x .

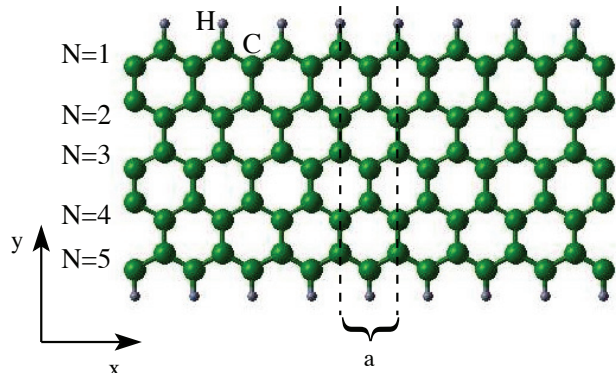


Figure 1: (color online) A mono-hydrogenated ribbon of width $N=5$ along y . The system is periodic only along x and the dashed lines delimit the periodic unit cell of length a .

The spin density of two stable magnetic states have been found; an *antiferromagnetic* (AF) state in which the spin localised on the edges is anti-parallel, Fig 2(a), and a *ferromagnetic* state in which it is parallel, Fig. 2(b).

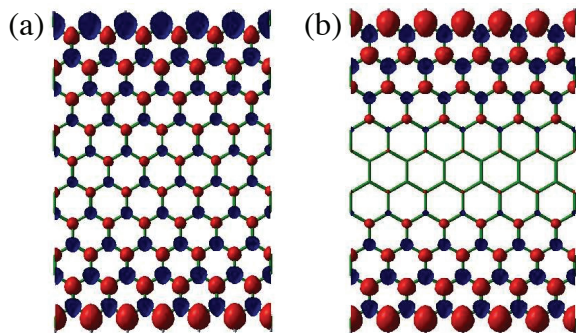


Figure 2: (color online) Isovalue surfaces of the spin density for the antiferromagnetic case (a) and ferromagnetic case (b). The red surfaces represents spin up density and the blue surface spin down density. The range of isovalue is $[-0.28:0.28] \mu_B/\text{\AA}^3$ in case (a) and $[-0.09:0.28] \mu_B/\text{\AA}^3$ in case (b).

The energy difference between the non-magnetic and the antiferromagnetic states, plotted in Fig. 3, is a measure of the strength of the magnetic instability. The

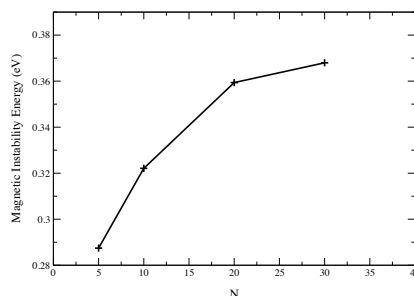


Figure 3: The energy difference (per unit cell) between the non-magnetic and antiferromagnetic case as a function of N .

stabilisation is larger for wider ribbons and converges to about 0.38 eV per unit cell at $N \sim 30$.

In the ground state AF configuration opposite spin polarisation on neighboring sites localises the electrons in singlet pairing between the two sublattices and a band gap opens at $k = \frac{2}{3}\frac{\pi}{a}$, where the valence and conduction bands of graphene are degenerate. The electronic ground state of a mono-hydrogenated ribbon of finite width is therefore insulating. As the width increases, the band gap tends to zero following an algebraic decay of the type $1/N$. The band gap vanishes, within room temperature thermal energy, when $N \simeq 400$, i.e., for an 80 nm wide ribbon. This length scale could be reached by the nanotechnology industry in the future with the synthesis of single, relatively thin sheets of nanographite [4].

4 ARRAYS of POINT DEFECTS

The representative point defect adopted here is a carbon vacancy in which, due to steric hinderance, two of the three dangling σ bonds are saturated with H-atoms. It is expected that the remaining dangling σ bond has no significant role to play in the conclusions drawn here.

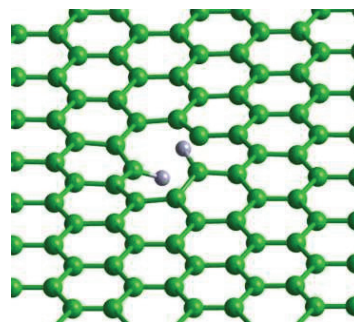


Figure 4: The structure of the defect considered in the present study.

Forming a periodic array of these defects reveals the localisation of spin at the defect and the mechanism for spin coupling between the defects. The resultant spin density for a defects spacing of 20 \AA is displayed in figure 5.

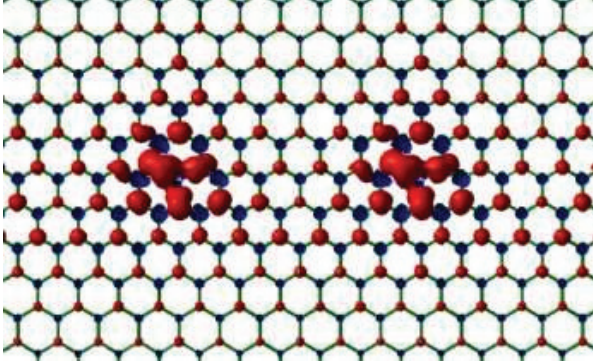


Figure 5: (color on line) Isovalue surfaces of the spin density of the graphene sheet with a defect separation of 20 \AA . The red (at $0.021 \mu_B/\text{\AA}$) and blue (at $-0.021 \mu_B/\text{\AA}$) isosurfaces represent the majority and minority spin densities, respectively.

The majority spin density within the defect is concentrated on the carbon atoms surrounding the vacancy and their second neighbours. The operation of the spin alternation rule, observed within graphene ribbons, in the spin polarised lattice is clearly visible [5], [4].

The electronic band structure of this state is shown in figure 6. The computed ground state is semiconducting. The presence of the defects and the magnetic ordering break the symmetry of the graphene π system, opening band gaps of 0.51 and 0.55 eV in the majority and minority spin band structures, respectively. The energy gap of the majority states is shifted upwards by about 0.20 eV with respect to the energy gap of the minority states, and the shape of the bands around the Fermi energy is markedly spin dependent. A strong spin asymmetry in the conductivity of the sheet is therefore to be expected.

Calculations at a variety of defect separations establish that the band gap scales as L^{-2} [5]. This decay law is consistent with that computed for graphene ribbons where the edges are line defects at which the spin moments localise and the band gap scales as L^{-1} with the ribbon width [4].

Although creating the particular defect structure studied here is not currently possible it is notable that there are now a number of techniques under development for generating and controlling the density of defects in a graphene sheet including the use of electron beams [6].

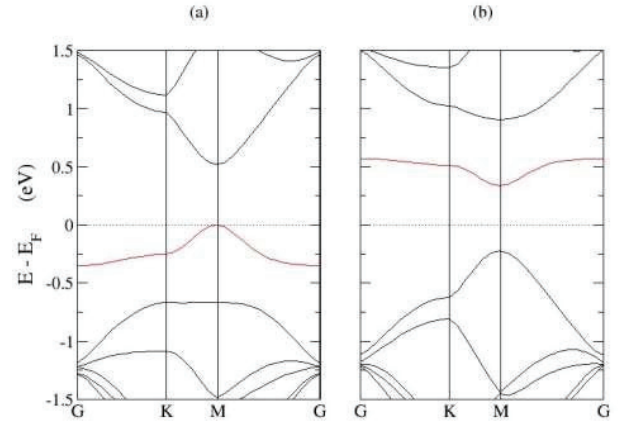


Figure 6: (color on line) The electronic energy bands of the majority (a) and minority (b) spin states of the ferromagnetic ground state in a defective graphene sheet with a defect separation of 20 \AA plotted with respect to the Fermi energy (E_F). The rather flat impurity bands near the Fermi energy, which are associated with the states localised at the defect, are indicated in red.

5 CONCLUSIONS

In conclusion, first principles calculations have been used to establish that the electronic structure of graphene ribbons with zig-zag edges is unstable with respect to a magnetic polarisation of the edge states. The calculated magnetic interaction of the edge states is remarkably long ranged. A band gap in the bulk of the ribbon exists in the antiferromagnetically aligned ground state with the size of the gap also displaying a very long range dependence on the ribbon width closing, at room temperature for ribbon widths exceeding 80nm . The mechanism for the opening of the band gap and the long range magnetic coupling is a spin alternation instability of the bipartite graphene lattice.

The introduction of a periodic array of point defects also generates localised magnetic moments and, through a very similar mechanism, can produce a semiconducting ferromagnetic state at room temperature for defect separations up to 20 \AA and thus for defect concentrations as low as $10^{13}/\text{cm}^2$. The energy gap and magnetic coupling depend strongly on defect concentration. We conclude that a doped or defective graphene sheet is a very promising material with an in built mechanism for tailoring properties for a variety of spintronics applications.

These results have direct implications for the control of the spin dependent conductance in graphitic nanoribbons using suitably modulated magnetic fields.

REFERENCES

- [1] Becke AD. A New Mixing of Hartree-Fock and Local Density-Functional Theories. *J Chem Phys.* 1993;98:1372.
- [2] Muscat J, Wander A, Harrison NM. On the prediction of band gaps from hybrid functional theory. *Chem Phys Letts.* 2001;342:397.
- [3] Dovesi R, Saunders VR, Roetti C, Orlando R, Zicovich-Wilson CM, Pascale F, et al. *CRYSTAL 2006 Users's Manual.* University of Torino; 2007.
- [4] Pisani L, Chan JA, Montanari B, Harrison NM. Electronic Structure and Magnetic Properties of Graphitic Ribbons. *Phys Rev B.* 2007;75:064418.
- [5] Pisani L, Montanari B, Harrison NM. A Defective Graphene Phase Predicted to be a Room Temperature Ferromagnetic Semiconductor. *New J Phys.* 2008;10:033002.
- [6] Warner JH, Rummeli MH, Ge L, Gemming T, Montanari B, Harrison NM, et al. Structural Transformations in Graphene Studied with High Spatial and Temporal Resolution. *Nature Nanotech.* 2009;4:500.